MPMI Vol. 36, No. 8, 2023, pp. 489–501, https://doi.org/10.1094/MPMI-12-22-0247-R

Wheat Pore-Forming Toxin-Like Protein Confers Broad-Spectrum Resistance to Fungal Pathogens in *Arabidopsis*

Lovepreet Singh,[1] Arunima Sinha,[1] Megha Gupta,[1] Shunyuan Xiao,[1,2] Rosemarie Hammond,[3] and Nidhi Rawat[1,†]

[1] Department of Plant Science and Landscape Architecture, University of Maryland College Park, MD 20742, U.S.A.
[2] Institute for Bioscience and Biotechnology Research, Rockville, MD 20850, U.S.A.
[3] Molecular Plant Pathology Laboratory, U.S. Department of Agriculture, Agricultural Research Service, Beltsville, MD 20705, U.S.A.

Accepted for publication 1 March 2023.

Fusarium head blight (FHB), caused by the hemibiotrophic fungus *Fusarium graminearum*, is one of the major threats to global wheat productivity. A wheat pore-forming toxin-like (PFT) protein was previously reported to underlie *Fhb1*, the most widely used quantitative trait locus in FHB breeding programs worldwide. In the present work, wheat PFT was ectopically expressed in the model dicot plant *Arabidopsis*. Heterologous expression of wheat PFT in *Arabidopsis* provided a broad-spectrum quantitative resistance to fungal pathogens including *F. graminearum*, *Colletotrichum higginsianum*, *Sclerotinia sclerotiorum*, and *Botrytis cinerea*. However, there was no resistance to bacterial or oomycete pathogens *Pseudomonas syringae* and *Phytophthora capsici*, respectively in the transgenic *Arabidopsis* plants. To explore the reason for the resistance response to, exclusively, the fungal pathogens, purified PFT protein was hybridized to a glycan microarray having 300 different types of carbohydrate monomers and oligomers. It was found that PFT specifically hybridized with chitin monomer, *N*-acetyl glucosamine (GlcNAc), which is present in fungal cell walls but not in bacteria or oomycete species. This exclusive recognition of chitin may be responsible for the specificity of PFT-mediated resistance to fungal pathogens. Transfer of the atypical quantitative resistance of wheat PFT to a dicot system highlights its potential utility in designing broad-spectrum resistance in diverse host plants.

Keywords: *Arabidopsis*, bacteria, broad-spectrum resistance (BSR), fungal pathogen, heterologous expression, oomycete, pore-forming toxin-like (PFT) protein, wheat *Fhb1*

Plants encounter various microbial pathogens in their environment, including fungi, bacteria, viruses, and nematodes. Plant resistance to pathogens is conferred by an elaborate, sophisticated, and multilayered system of defense (Dangl et al. 2013; Dodds and Rathjen 2010; Zhou and Zhang 2020). The first tier of plant defense is pathogen-associated molecular pattern (PAMP)-triggered immunity (PTI) mediated by the pattern recognition receptors on the cell surface and occurs during the early phase of host-pathogen interactions. The second tier of plant defense is the effector-triggered immunity mediated by plant resistance (*R*) genes, most of which encode cytoplasmic receptor proteins with nucleotide-binding leucine-rich repeat (NLR) domains (Jones and Dangl 2006; Zhou and Zhang 2020). The resistance genes other than the *R* genes are often referred to as atypical resistance genes (Sinha et al. 2022; Yan et al. 2022; Zhao et al. 2018). The atypical resistance genes are diverse and may confer a broad-spectrum resistance (BSR) against two or more pathogen species or even against the majority of races of the same species (Kou and Wang 2010; Li et al. 2020). Given their wider applicability, such atypical BSR genes are ideal candidates for engineering disease resistance in crop plants (Li et al. 2020; Ning and Wang 2018). A better mechanistic understanding of the modes of action of the atypical BSR genes will facilitate their wider usage in plant breeding and agriculture (Tian et al. 2020; Zhao et al. 2018).

Wheat is one of the most important food crops cultivated globally (Bentley et al. 2022; FAOSTAT 2020). Fusarium head blight (FHB), caused by the ascomycete fungus *Fusarium graminearum*, is one of the most devastating diseases of wheat (Goswami and Kistler 2004; McMullen et al. 2012). Several quantitative trait loci (QTL) providing resistance to FHB have been mapped in wheat, out of which *Fhb1*, located on chromosome 3B of wheat cultivar Sumai 3, is the most widely deployed QTL in wheat cultivars worldwide (Buerstmayr et al. 2020). Previously, using mutation analysis, gene silencing, and overexpression, Rawat et al. (2016) showed a pore-forming toxin-

[†]Corresponding author: N. Rawat; nidhirwt@umd.edu

L. Singh and A. Sinha contributed equally.

Author contributions: L.P.S. generated transgenic *Arabidopsis* events, conducted *Fusarium graminearum* assays, and carried out the protein work, A.S. and M.G. conducted assays with other necrotrophic and hemi-biotrophic fungal pathogens as well as bacterial and oomycete pathogens, S.X. conducted powdery mildew screening of the transgenic plants, R.H. helped with the protein work, N.R. planned the research, arranged funding, and wrote the manuscript with L.P.S. and A.S.

Funding: This work was funded by National Institute of Food and Agriculture award 2020-67013-32558, National Science Foundation award 1943155, and United States Wheat and Barley Scab Initiative award 59-0206-2-130.

e-Xtra: Supplementary material is available online.

The author(s) declare no conflict of interest.

like (PFT) protein to underlie the *Fhb1*-mediated resistance in wheat. PFT is a chimeric plant lectin with two amaranthin domains (agglutinin domains of *Amaranthus caudatus*) and one bacterial toxin domain of the aerolysin pore-forming toxin family (Rawat et al. 2016). Lectins are proteins that bind reversibly to specific carbohydrates and perform diverse biological functions in organisms (Franck et al. 2018; Peumans and Van Damme 1995; Tsaneva and Van Damme 2020). Lectins with amaranthin domain have been reported to provide resistance against insects (Wu et al. 2006; Xin et al. 2011) and bacteria (Chavonet et al. 2022). Chimeric lectins with domain architecture of two amaranthin domains and an aerolysin pore-forming toxin domain have been partially characterized in wheat (Puthoff et al. 2005), flax (Faruque et al. 2015), cucumber (Dang and Van Damme 2016), and *Rumex acetosa* plants (Manzano et al. 2017). However, the range and mode of action of wheat PFT against fungal pathogens is not known yet.

The goal of the present work was to test if the wheat PFT-mediated resistance could be ectopically transferred to a dicot plant system. If yes, was the resistance conferred specific to *F. graminearum* or was it broader against several fungal pathogens? Does PFT provide resistance against bacterial and oomycete pathogens? If differences in response to various classes of pathogens occur, what could be the underlying reasons?

Results

Phylogenetic analysis of PFT.

Phylogenetic analysis of wheat PFT across multiple monocots and dicot plant species revealed scattered distribution of PFT orthologs in them. In monocots, PFT orthologs were found present in *Zea mays*, *Hordeum vulgare*, and *Brachypodium distachyon*, whereas they were absent in *Oryza sativa* and *Musa acuminate* (Supplementary Fig. S1). Among the eudicots searched, *Vitis vinifera*, *Ricinus communis*, *Prunus armeniaca*, *Gossypium hirsutum*, and *Beta vulgaris* showed the presence of PFT orthologs, whereas *Solanum lycopersicum*, *Solanum tuberosum*, *Populus deltoids*, *Phaseolus vulgaris*, *Medicago truncatula*, *Glycine max*, and *Arabidopsis thaliana* lacked PFT orthologs (Supplementary Fig. S1). The absence of PFT orthologs in *A. thaliana* makes this model plant more suitable to study the heterologous expression of PFT and generate stable transgenic lines.

Generation of GFP:PFT transgenics in *Arabidopsis*.

Previous studies by Urban et al. (2002) and Chen et al. (2006) have shown *Arabidopsis* ecotype Landsberg erecta (Ler) to be more susceptible to *F. graminearum* infection than the most frequently used ecotype in plant molecular biology, i.e., Columbia 0. Therefore, in this study, we used *Arabidopsis* ecotype Ler to test the response of wheat PFT to *F. graminearum* and other pathogens upon its ectopic expression. For generating PFT-expressing transgenic plants in *Arabidopsis*, we developed a fusion construct with enhanced green fluorescent protein (GFP) domain fused at the N terminus of the wheat PFT coding sequence. The expression of PFT was driven by the 35S cauliflower mosaic virus (CaMV) promoter and kanamycin resistance was used as a selectable marker (Fig. 1A). The selection efficiency with kanamycin resistance ranged from 2 to 4% in the T_1 generation. Kanamycin-resistant T_1 plants were further screened for GFP signal under an epifluorescence microscope (Fig. 1C). Fifty percent of the kanamycin-resistant T_1 plants had a GFP signal. The remaining 50% with no GFP signal were discarded. T_1 plants with GFP signal were grown for seed increase and their T_2 families were tested for segregation. Ultimately, two independent nonsegregating homozygous T_2 families (AT46 and AT58) were used for disease bioassays in this study. Analysis of the relative expression of PFT using reverse transcription-quantitative PCR (RT-qPCR) showed a high level of PFT expression in both the T_2 transgenic families (AT46 and AT58) (Fig. 1B).

The fusion protein in the selected T_2 plants was confirmed via Western blot analysis with an anti-GFP antibody (Fig. 1D). A specific band of approximately 79 kDa was detected in the GFP:PFT-fused transgenic plants. The size of PFT in sodium dodecyl sulfate-polyacrylamide gel electrophoresis (SDS-PAGE) is approximately 52 kDa and the size of GFP is approximately 27 kDa. Therefore, the presence of a unique approximately 79 kDa band only in transgenics and not in wild type (WT) confirmed the production of complete fusion protein in GFP:PFT transgenics.

In addition to T_2 families, four different T_3 families derived from the selected T_2 plants were further selected and screened for GFP signal and were assessed for their response to different fungal pathogens.

PFT confers resistance to *F. graminearum* in *Arabidopsis* detached leaf assays and in-planta floral assays.

The selected GFP:PFT transgenic plants were used for both leaf and floral bioassays with *F. graminearum*. Detached leaf assays were performed twice on four fully expanded leaves taken from the rosettes of 10 transgenic plants when they were 4 to 5 weeks old. At 5 days postinoculation (dpi), chlorosis, water-soaking, and lesions were observed in the infiltrated area WT controls (Fig. 2A). In contrast, the T_2 (AT46 and AT58) transgenic plants expressing PFT exhibited smaller chlorotic areas, water-soaking and lesion symptoms (Fig. 2A). Further, new sets of detached infected leaves were studied with trypan blue staining to observe cell death and fungal progression in them (Takemoto et al. 2005). At 4 dpi with *F. graminearum*, dense clusters of blue-stained plant cells were observed in the WT Ler leaves, indicative of extensive cell death, while both the AT46 and AT58 transgenic plants showed very few scattered patches of blue-stained cells (Fig. 2B). The containment of cell death in the transgenic plants indicates a moderate to high degree of resistance to *F. graminearum* provided by the ectopic PFT expression in the transgenic Ler plants.

The disease severity (DS) index was calculated, on infected leaves 5 dpi, according to Chen et al. (2006). The mean DS index score for WT Ler was found to be 75%, while for GFP:PFT transgenics, it was 58% for AT58 and 63% for AT46, which was significantly lower at 0.01 and 0.005 significance levels, respectively (Fig. 2D). Using a more sensitive assay, we measured the biomass of *F. graminearum* on the infected leaves, based on the DNA quantity of a trichothecene biosynthesis pathway gene, *Tri6*. GFP:PFT transgenic plants had significantly lower ($P < 0.001$) *Tri6* DNA compared with WT (Fig. 2E). Compared with WT, *Tri6* DNA quantity in AT46 and AT58 was 58 and 67% lower, respectively. Taken together, PFT ectopic expression significantly reduced *F. graminearum* infection in inoculated *Arabidopsis* leaves.

Since *F. graminearum* infects wheat at the flowering stage in natural conditions, we further analyzed our transgenic *Arabidopsis* families to test if PFT expression confers in planta floral disease resistance. We spray-inoculated WT and transgenic T_2 plants with *F. graminearum* spores, following Urban et al. (2002). After 8 days of inoculation, in the WT plants, flowers completely collapsed with necrotic peduncle and extensive necrosis of young siliques occurred (Fig. 2C). On the other hand, the PFT transgenics had an intact peduncle and no silique necrosis was observed. To quantify the disease response in the floral tissue, we measured *F. graminearum* fungal biomass by measuring the DNA quantity of the fungal *Tri6* gene at 8 dpi (Fig. 2F). *Tri6*-based DNA quantification showed 51 and 70%

lower *F. graminearum* biomass in AT46 and AT58, respectively, compared with the WT, which was significantly (P value $<$ 0.05) lower in both the transgenic families compared with WT. These results demonstrate that wheat PFT ectopic expression in *Arabidopsis* provided resistance in the floral tissue similar to that in wheat spikes in its natural form.

PFT confers resistance to several fungal pathogens in T_2 transgenic *Arabidopsis* plants.

To study if the resistance conferred by PFT is broad-spectrum against fungal pathogens, we challenged the transgenic plants along with the WT plants with the following fungal pathogens of *Arabidopsis*: *Colletotrichum higginsianum*, *Botrytis cinerea*,

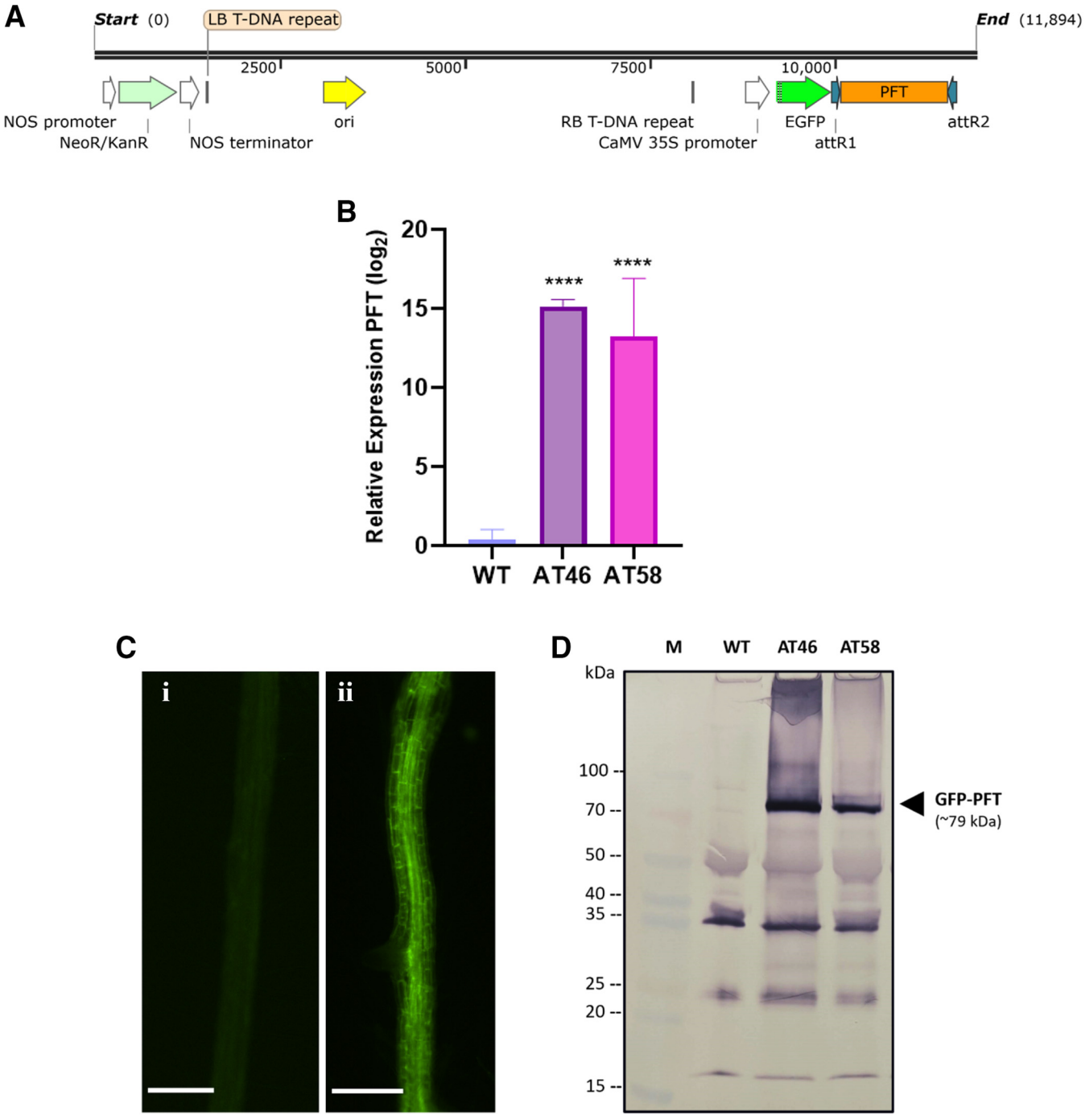

Fig. 1. Generating and selecting GFP:PFT transgenics in *Arabidopsis*. **A,** Map of pore-forming toxin-like (PFT) protein cloned in pK7FWG2. Scale units in base pairs (bp). LB = Luria-Bertani; NOS = nopaline synthase. **B,** Relative expression of PFT in T_2 *Arabidopsis* transgenic lines AT46 and AT58. Relative expression of the PFT gene was measured by the $2^{-\Delta\Delta CT}$ method by normalizing data with the *Arabidopsis UBC* gene and using wild type (WT) as reference, using reverse transcription-quantitative PCR. Data represent means with standard error from five biological replicates. Asterisks (****) indicate statistical differences from WT at $P < 0.00001$. **C,** Screening of GFP:PFT transgenics using an epifluorescence microscope. Panel i shows WT *Arabidopsis* root and panel ii the root of a kanamycin-resistant, green fluorescent protein (GFP)-expressing T_2 *Arabidopsis* seedling. Scale bar = 50 µm. **D,** Western blot analysis of GFP:PFT expressed in *Arabidopsis* transgenic plants. The membrane was probed with anti-GFP antibody followed by anti-goat anti-rabbit immunoglobulin G and was detected using alkaline phosphate-based detection. An equal amount of soluble protein was loaded in each lane. M is the protein marker, WT is WT *Arabidopsis* Ler, and AT46 and AT58 are T_2 *Arabidopsis* Ler families expressing GFP:PFT. Arrowhead indicates GFP:PFT fusion protein.

and *Sclerotinia sclerotiorum*. Detached leaf assays were performed on leaves from ten 4- to 5-week-old plants, each with the three fungal pathogens. Response of GFP:PFT transgenics to *C. higginsianum*, a well-known hemibiotrophic fungus was assessed based on visual symptoms and fungal biomass. WT *Arabidopsis* leaves had larger chlorotic lesions, while GFP:PFT T_2 transgenic plants showed very small lesions at the point of inoculation (Fig. 3A). Mean DS index scores were 35% and 10 to 12% in WT Ler and the two transgenic families, respectively (Fig. 3B). *C. higginsianum* biomass was then quantified by monitoring the relative DNA quantification of the *ITS2* (internal transcribed spacer) gene. The *C. higginsianum* biomass was fourfold less in the transgenic plants compared with WT (Fig. 3C). Statistically, significantly ($P < 0.001$) lower disease severity and lower pathogen growth ($P < 0.05$) demonstrate that PFT confers resistance against *C. higginsianum*.

Next, we inoculated the transgenic families as well as WT Ler *Arabidopsis* plants with *S. sclerotiorum*. In the *S. sclerotiorum* infection assay, AT46, and AT58 T_2 transgenic *Arabidopsis* leaves showed smaller necrotic lesions compared with WT (Fig. 3D) 48 h postinoculation (hpi), with the mean DS index for WT (38%) significantly higher than AT46 (18%) and AT58 (26%) transgenic families (Fig. 3E). For more precise disease assessment, we then measured the fungal biomass by monitoring the DNA copy number of *Tubulin*. Both T_2 transgenic families had significantly ($P < 0.01$) lower *S. sclerotiorum* biomass than WT (Fig. 3F). Compared with WT, *S. sclerotiorum* biomass was 14-fold and approximately eightfold lower in AT46 and AT58, respectively.

In the *B. cinerea* assays, the mean DS index of WT Ler was 25%, which was significantly ($P < 0.05$) higher than the GFP:PFT transgenic families AT46 (9%) and AT58 (12%) (Fig. 3G and H). The DNA quantity of *Cutinase A* was measured to evaluate *B. cinerea* biomass in the infected leaves 5 dpi, which showed that, compared with WT, both the T_2 transgenic families had significantly reduced fungal biomass (Fig. 3I).

Response of the T_3 families to the hemibiotrophic and necrotrophic fungal pathogens.

We further tested the stability of PFT expression and the response to fungal infection in four T_3 transgenic plant families (AT67, AT68, AT69, and AT70) derived from the tested T_2 families (two each from AT46 and AT58), using *F. graminearum*, *C. higginsianum*, *S. sclerotiorum*, and *B. cinerea*. The T_3 plants were selected for their kanamycin resistance and GFP signal. The detached leaf assays showed WT Ler leaves to contain larger chlorotic lesions, as compared with the T_3 transgenic families, after 5 dpi with *F. graminearum*, *C. higginsianum*, and *B. cinerea* and 48 hpi with *S. sclerotiorum* (Fig. 4A). Mean DS index scores for WT Ler ranged between 45 to 75%, while the

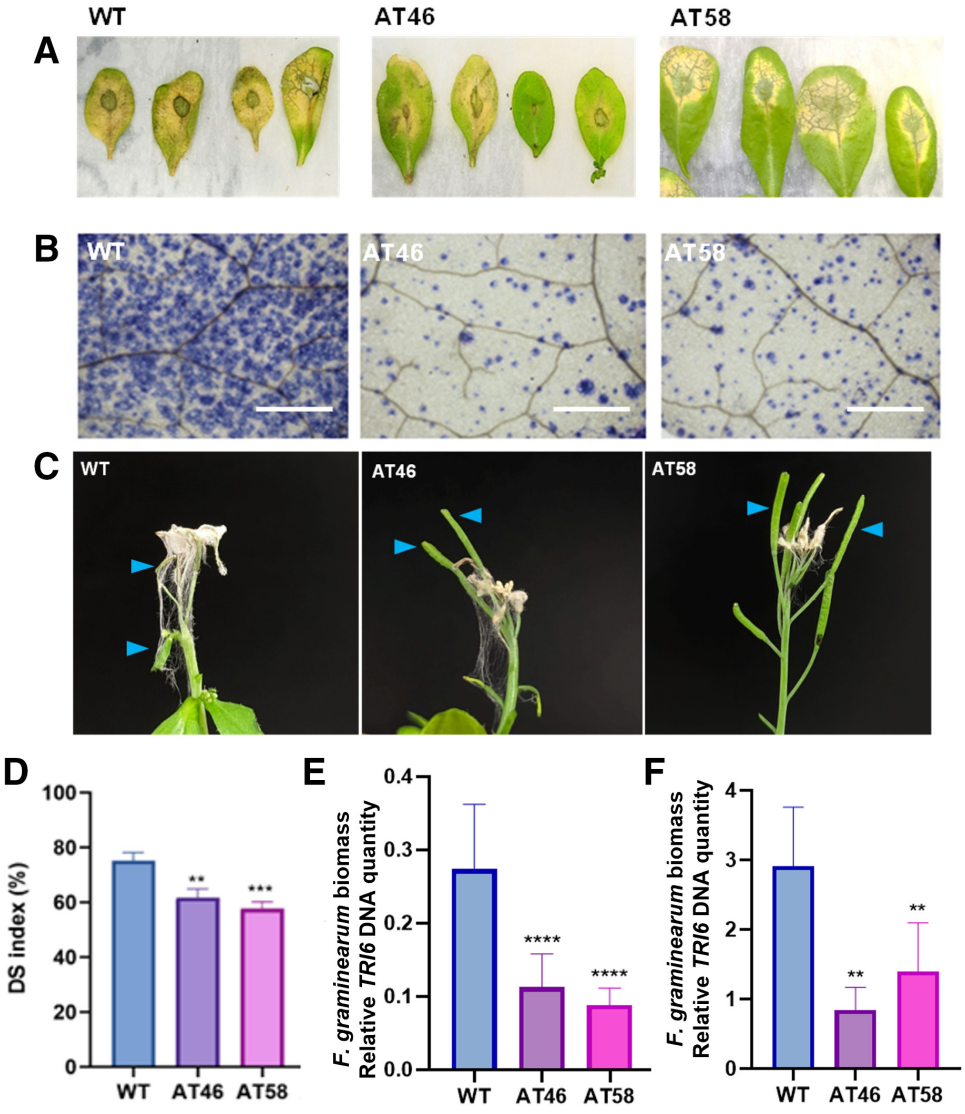

Fig. 2. Detached leaf assay and floral assay of wild type (WT) and transgenic T_2 *Arabidopsis* plants expressing GFP:PFT. **A,** Disease symptoms observed 5 days postinoculation (dpi) of WT and T_2 *Arabidopsis* leaves with *Fusarium graminearum*. **B,** Trypan blue staining to visualize dead cells and fungal mycelium in WT and transgenic *Arabidopsis* leaves after 4 dpi with *F. graminearum*. Scale bar = 50 µm. **C,** Disease symptoms observed 8 dpi of WT and T_2 *Arabidopsis* flowers with *F. graminearum*. Arrowheads (in blue) point to necrotic siliques growing in WT control as compared with AT46 and AT58 plants. **D,** Disease severity (DS) index of WT and transgenic lines measured 5 dpi with *F. graminearum*. **E,** Fungal biomass of *F. graminearum* detected by quantitative real-time PCR (qPCR) on inoculated leaves 3 dpi. Relative DNA quantity of the *TRI6* gene was measured, using the $2^{-\Delta CT}$ method, by normalizing data with the *Arabidopsis UBC* gene. **F,** Fungal biomass of *F. graminearum* detected by qPCR on inoculated florets 8 dpi. Relative DNA quantity of *TRI6* gene was measured, using the $2^{-\Delta CT}$ method, by normalizing data with the *Arabidopsis UBC* gene. WT = WT *Arabidopsis* Ler, AT46 and AT58 are T_2 *Arabidopsis* Ler families expressing GFP:PFT. Data represent means with standard error from four biological replicates. One, two, or three asterisks (*, **, or ***) indicate statistical differences from WT at $P < 0.05$, $P < 0.01$, or $P < 0.001$, respectively.

majority of GFP:PFT T_3 transgenics had mean DS index significantly lower for all four of the tested fungal pathogens (Fig. 4B). Finally, fungal biomasses were quantified by monitoring the DNA quantity of *Tri6*, *ITS2*, *Tubulin*, and *Cutinase A* in WT Ler and T_3 transgenic families inoculated with *F. graminearum*, *C. higginsianum*, *S. sclerotiorum*, and *B. cinerea*, respectively, which showed significant reduction in fungal biomass ($P < 0.05$) with all four fungal pathogen assays (Fig. 4C). Overall, the ectopic expression of PFT in T_2 and T_3 *Arabidopsis* transgenic plants significantly reduced disease severity and conferred a quantitative BSR against all the tested fungal pathogens.

PFT does not confer resistance to bacteria and oomycete pathogens.

After confirmation of the resistance of PFT *Arabidopsis* transgenics to the different fungal pathogens, we further tested the T_2 transgenic plants AT46 and AT58 for their response to the bacterial pathogen *Pseudomonas syringae* pv. *tomato* DC3000. To test this, we performed in-planta as well as detached-leaf assays. For in-planta assays, we syringe-infiltrated WT Ler and GFP:PFT T_2 transgenic leaves expressing PFT with 1×10^8 colony-forming units (CFU) of bacterial inoculum per milliliter or 10 mM $MgCl_2$ with 0.02% Silwet L-77 for mock. Detached-leaf assays were performed by spraying the bacterial inoculum on the WT Ler and T_2 transgenic leaves. Three days after inoculation, it was observed that mock inoculations did not show any visual symptoms whereas WT and both the T_2 transgenic families showed similar water-soaked lesions with bleaching and cell death in both the in-planta and detached-leaf assays (Fig. 5A and B). Further, bacterial biomass was calculated in terms of CFU cm^{-2} leaf and it was found that for syringe infiltration in planta assay, the transgenic plants as well as WT had approximately 3.57E + 06 CFU cm^{-2} leaf (Fig. 5C) while spray inoculated detached WT as well as the transgenic plants showed 6.56E + 06 CFU cm^{-2} leaf (Fig. 5D). Both in planta as well as detached leaf assays for bacterial quantification revealed no significant difference between WT and transgenic plants in the disease assessment for *P. syringae* infection revealing that PFT is not effective in conferring resistance against bacterial pathogens.

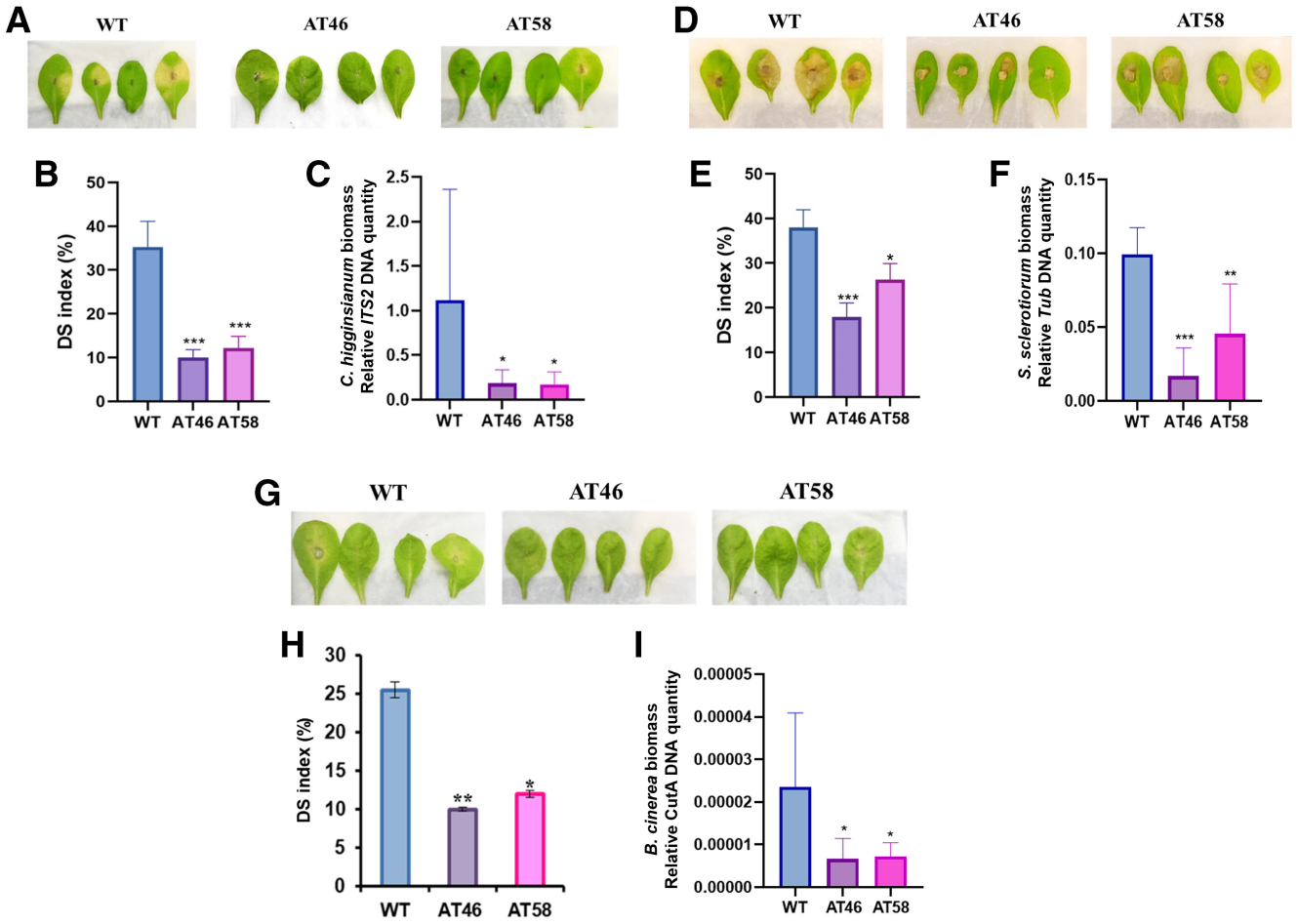

Fig. 3. Disease assessment of wild type (WT) and transgenic T_2 *Arabidopsis* plants expressing GFP:PFT. **A,** Disease symptoms observed 5 days postinoculation (dpi) of WT and T_2 *Arabidopsis* leaves with *Colletotrichum higginsianum*. **B,** Disease severity (DS) index of WT and transgenic lines measured 5 dpi with *C. higginsianum*. **C,** Fungal biomass of *C. higginsianum* detected by quantitative real-time PCR (qPCR) on inoculated leaves 5 dpi. Relative DNA quantity of the *ITS2* gene was measured, using the $2^{-\Delta CT}$ method, by normalizing data with the *Arabidopsis UBC* gene. **D,** Disease symptoms observed 48 h postinoculation (hpi) of WT and T_2 *Arabidopsis* leaves with *Sclerotinia sclerotiorum*. **E,** DS index of WT and transgenic lines measured 48 hpi with *S. sclerotiorum*. **F,** Fungal biomass of *S. sclerotiorum* detected by quantifying Tubulin DNA, using qPCR on inoculated leaves 48 hpi. The relative DNA quantity of *Tubulin* gene was measured, using the $2^{-\Delta CT}$ method, by normalizing data with the *Arabidopsis UBC* gene. **G,** Disease symptoms observed 5 dpi of WT and T_2 *Arabidopsis* leaves with *Botrytis cinerea.* **H,** DS index of WT and transgenic lines measured 5 dpi with *B. cinerea*. **I,** Fungal biomass of *B. cinerea* detected by quantifying *CutinaseA* DNA, using qPCR on inoculated leaves 5 dpi. The relative DNA quantity of the *CutinaseA* gene was measured, using the $2^{-\Delta CT}$ method, by normalizing data with the *Arabidopsis UBC* gene. WT is WT *Arabidopsis* Ler, and AT46 and AT58 are T_2 *Arabidopsis* Ler families expressing GFP:PFT. Data represents mean with standard error from 10 biological replicates. Bars with one, two, or three asterisks (*, **, or ***) indicate that corresponding data is statistically different from WT at $P < 0.05$, $P < 0.01$, or $P < 0.001$, respectively.

Further, we tested whether PFT is effective in conferring resistance to the oomycete pathogen *Phytophthora capsici.* WT Ler and GFP:PFT T2 transgenic *Arabidopsis* leaves were inoculated with 5×10^5 zoospores per milliliter of *P. capsici* and disease evaluation was done at 3 dpi. Both WT and transgenics showed chlorotic lesions at the site of inoculation to the same extent visually (Fig. 6A) with an average DS Index of ~45% for WT, AT46 and AT58 transgenic families (Fig. 6B). Quantification of the *P. capsici* biomass by measuring relative DNA quantity of *ITS* gene in leaves of WT Ler and the transgenic *Arabidopsis* at 3 dpi by qPCR revealed statistically similar levels of the pathogen in all three of them (Fig. 6C). Similar to bacteria, these results elucidated that PFT is not effective in imparting resistance against oomycete pathogens, defining its defensive role against only fungal pathogens.

PFT binds to chitin monomer GlcNAc.

Domain analysis of PFT protein shows that it is a chimeric lectin with two agglutinin domains and a toxin domain. Lectins are proteins that bind to specific carbohydrate molecules (De Coninck and Van Damme 2021; Van Damme et al. 2004). Based on our disease assay results, we hypothesized that the agglutinin domains in the PFT protein may be explicitly binding to a specific carbohydrate present in the fungal pathogens and absent in bacterial and oomycete pathogens. To test this hypothesis, we cloned separately the full-length PFT and its constituent domains agglutinin and ETX (epsilon toxin) in binary vector pGWB402 with a CaMV 35S promoter. His tags (6X) were attached to the N-terminus of the proteins and domains and *Agrobacterium* sp. strain GV3101 was used for transient expression of the different constructs in *N. benthamiana*. PFT protein and the ETX domain were isolated and confirmed on Western blot for size and

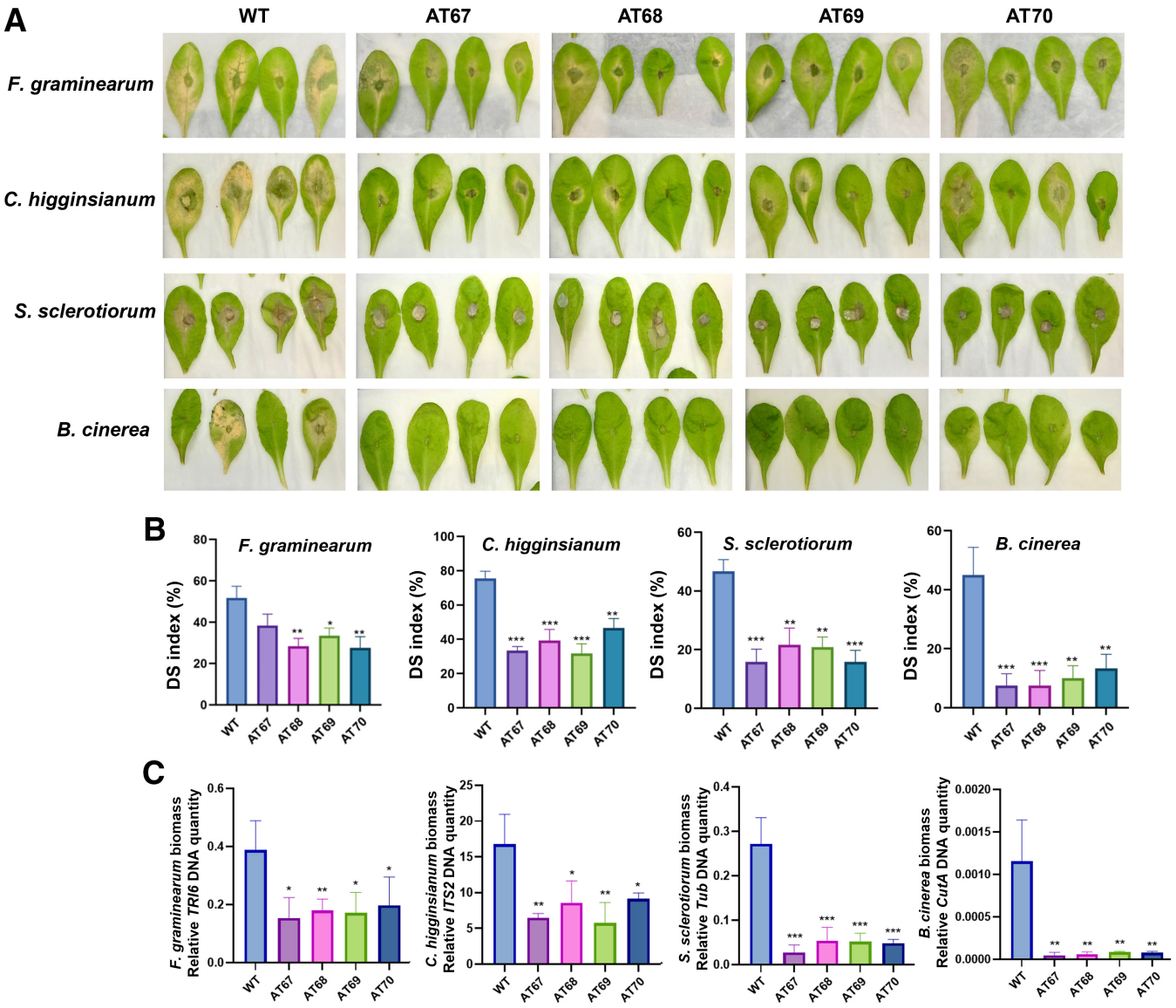

Fig. 4. Disease assessment of wild type (WT) and transgenic T_3 *Arabidopsis* plants expressing GFP:PFT. **A,** Disease symptoms observed and **B,** Disease severity (DS) index of detached WT and T_3 *Arabidopsis* leaves 5 days postinoculation (dpi) with *Fusarium graminearum*, *Colletotrichum higginsianum*, and *Botrytis cinerea* and 48 h postinoculation (hpi) with *Sclerotinia sclerotiorum.* **C,** Fungal biomass of *F. graminearum*, *C. higginsianum*, *S. sclerotiorum*, and *B. cinerea* detected by quantitative real-time PCR. Relative DNA quantity of *Tri6*, *ITS2*, *Tubulin*, and *CutinaseA* genes was measured, using the $2^{-\Delta CT}$ method, by normalizing data with the *Arabidopsis UBC* gene. WT is WT *Arabidopsis* Ler, and AT67, AT68, AT69, and AT70 are T_3 *Arabidopsis* Ler families expressing GFP:PFT. Data represents means with standard error from 10 biological replicates. Bars with one, two, or three asterisks (*, **, or ***) indicates that corresponding data is statistically different from WT at $P < 0.05$, $P < 0.01$, or $P < 0.001$, respectively.

quantity (Fig. 7A). The agglutinin domain was present in the insoluble fraction and, thus, could not be isolated for the downstream experiments. The isolated His6-PFT and His6-ETX were affinity-purified.

The purified proteins were hybridized at a concentration of 2 μg/ml with the RayBio Glycan Array 300 according to the manufacturer protocol. The array contained 300 glycan (carbohydrate monomers and oligomers) spots in triplicate copies, 12 positive control spots, and six negative control spots. As both His6-PFT and His6-ETX were isolated and affinity-purified using the same method, they were expected to have common background proteins in their solution. Therefore, His6-ETX was used as a negative control for deducing the glycan-binding affinity of His6-PFT protein. The experiment was conducted in two independent copies. The 2-μg/ml sample concentration provided good signal intensity to compare the relative differences in binding patterns of His6-PFT and His6-ETX. Of the 300 glycans tested, 11 showed strong and specific signals for His6-PFT (Fig. 7B). These glycans had relative fluorescent unit (RFU) values of more than 4,000, indicating a high binding affinity of only PFT to these 11 glycans (Fig. 7C). The results were in complete agreement between the two replicated experimental runs. Interestingly, all 11 glycans had one or multiple units of monosaccharide GlcNAc, which is the monomer of the fungal cell-wall component chitin (Fig. 7D). Furthermore, although in a comparatively lower RFU range (962 to 2,164), the binding affinity of His6-PFT was 26, 24, and 85% higher than His6-ETX for β-GlcNAc-Sp, GlcNAc-β-1,6-GlcNAc-β-Sp, and chitin-trisaccharide-Sp1 glycans, respectively. Glycan array screening indicated a PFT-specific affinity towards binding the fungal cell wall–specific

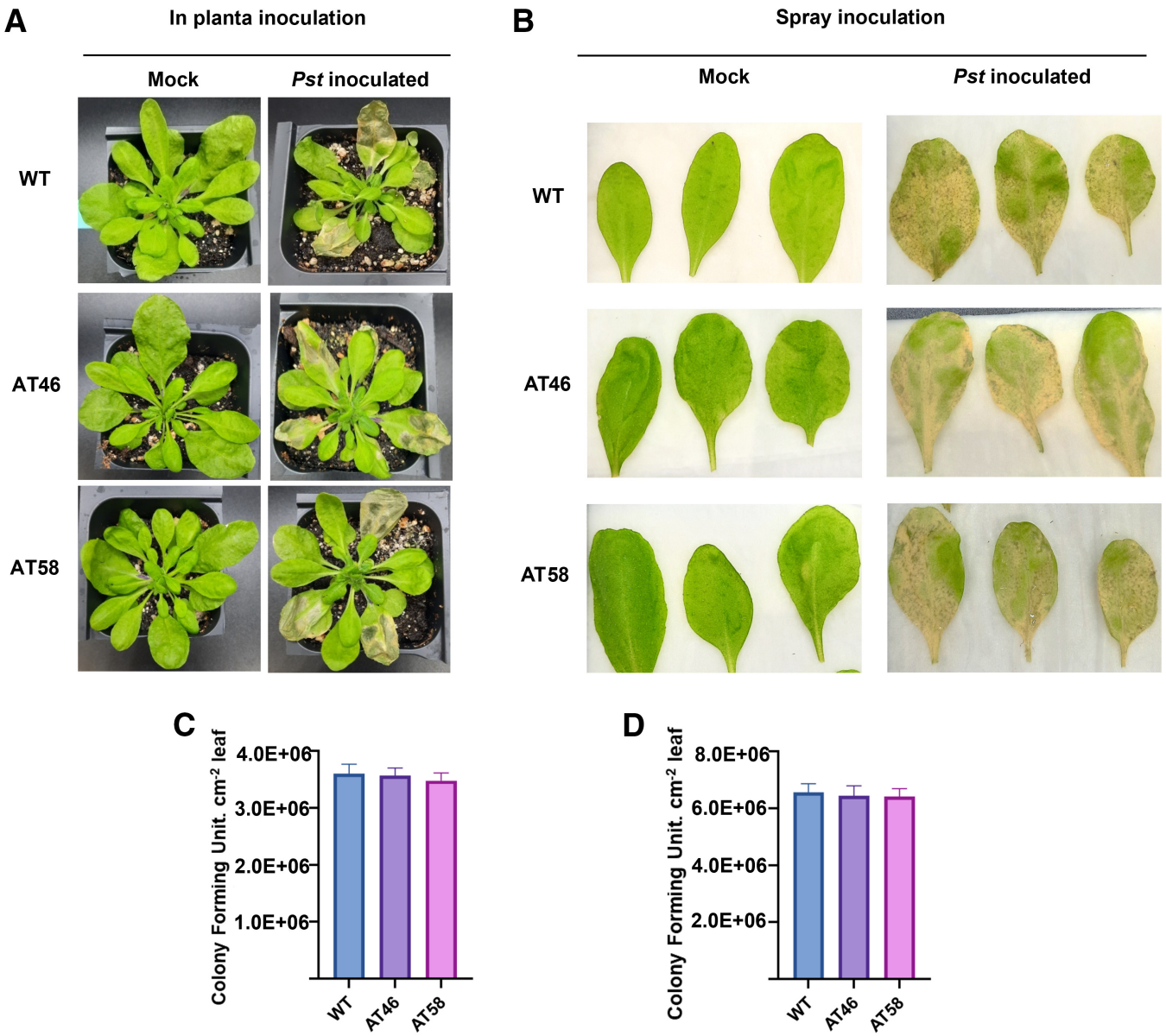

Fig. 5. Disease assessment of wild type (WT) and transgenic T_2 *Arabidopsis* plant families expressing GFP:PFT after bacterial *Pseudomonas syringae* pv. *tomato* DC3000 (*Pst*) infection. **A,** Disease symptoms recorded 3 days after syringe-infiltration with 1×10^8 CFU/ml of *Pseudomonas syringae* pv. *tomato* DC3000 in planta WT and T_2 *Arabidopsis* leaves. **B,** Disease symptoms recorded 3 days after spray-inoculation with 1×10^8 CFU/ml of *Pseudomonas syringae* pv. *tomato* DC3000 on detached WT and T_2 *Arabidopsis* leaves. **C,** *Pseudomonas syringae* pv. *tomato* DC3000 growth (colony-forming units per square centimeter [CFU/cm^2] of leaf) was quantified 3 days after syringe infiltration with 1×10^8 CFU per millimeter of *Pseudomonas syringae* pv. *tomato* DC3000 in planta WT and T_2 *Arabidopsis* leaves. Data represent means with standard error from six biological replicates. **D,** *Pseudomonas syringae* pv. *tomato* DC3000 growth was quantified (CFU per square centimeter) 3 days after spray inoculation with 1×10^8 CFU per milliliter of *Pseudomonas syringae* pv. *tomato* DC3000 on detached WT and T_2 *Arabidopsis* leaves. Data represent means with standard error from six biological replicates.

chitin carbohydrate monomers, which may explain the specific response to fungal pathogens.

Discussion

Breeding crop varieties with BSR to pathogens is a key objective of crop improvement programs. Most of the major resistance genes used in crop breeding are NLR immune receptors that recognize specific effectors (Avrs) of the pathogens. Although these NLR genes are highly effective, their resistance is limited to one or more specific races of the pathogen and their durability in the field is typically short due to emergence of variations in the Avrs in the pathogen populations (Ning and Wang 2018). The *Fhb1*-mediated resistance of wheat to *Fusarium* spp. is not a typical NLR-mediated resistance. Previously, Rawat et al. (2016) demonstrated a PFT-encoding gene to be a major underlying determinant of *Fhb1*-mediated resistance. PFT is a chimeric lectin protein with two *Amaranthus caudatus* agglutinin domains and a bacterial pore-forming toxin domain (Rawat et al. 2016). In the present study, we characterized the ability of wheat PFT to confer BSR against several fungal pathogens in a dicot model plant system.

Based on the phylogenetic analysis, it is interesting to note that the dicot model plant *Arabidopsis* does not have any homolog or ortholog of wheat PFT in its genome. Wheat PFT was able to function and provide resistance in a dicot plant background, in which it is not present naturally, indicating toward either a resistance mechanism independent of extensive signaling pathways or recruitment of conserved defense players in the model dicot system towards resistance. Moran et al. (2012) studied the recurrent horizontal transfer of bacterial toxin genes to eukaryotes and concluded that members of the aerolysin pore-forming toxin family have undergone frequent horizontal gene transfers (HGT) to eukaryotes. They suggest that such gene families that are evolutionarily maintained after HGT in their new environment are most likely self-contained units and do not need other protein complexes or complicated pathways to function. However, more follow-up experiments are needed to conclude the extent of involvement of salicylic acid, jasmonic acid, and ethylene defense response pathways in the wheat-PFT-mediated resistance. Nevertheless, the resistance response of wheat PFT in a dicot system highlights its potential utility as an atypical BSR gene against fungal pathogens in multiple monocot and dicot crop plants.

PFT transgenics had significantly reduced disease severity and fungal biomass accumulation for the four fungal pathogens tested, showing that wheat PFT provides a BSR against a wide range of fungal pathogens. However, it was not found to be effective in imparting resistance against bacterial and oomycete pathogens, which suggests the selectivity and specificity of this protein in recognizing the fungal pathogens. To investigate the specific recognition of the fungal pathogens, we hybridized purified PFT proteins with an array of 300 different glycans. The specific binding of PFT to glycans containing single to multiple monomers of GlcNAc, which is the monomer of chitin, supports our hypothesis of chitin-specific binding of PFT to underlie its resistance to a wide range of fungal pathogens. Fungal cell walls are known to have chitin as one of their major constituents, whereas bacterial and oomycete pathogens do not have chitin in their cell walls (Bartnicki-García 1968; Goldman and Branstrom 1999; Hardham 2007). Based on this knowledge, the specificity of fungal recognition by PFT can be credited to chitin, which is exclusive to the fungal cell walls, among the three types of pathogens.

Lectin proteins are known to reversibly bind to specific carbohydrates and have been reported to have a role in plant immunity, stress signaling, and defense (De Coninck and Van Damme 2021; Peumans and Van Damme 1995). Lectin domains are important constituents of the lectin-receptor-like kinase (LecRLK) family in the PTI defense mechanism of plants (Couto and Zipfel 2016; Vaid et al. 2013). The LecRLKs have three domains: an extracellular lectin domain, a transmembrane domain, and a kinase domain (Sun et al. 2020; Zipfel 2014). The extracellular lectin domain is variable and serves as sensor of the PAMPs based on their specific binding affinity to different carbohydrate molecules, whereas the latter two domains of the LecRLKs are more conserved (Zipfel 2014). In the case of wheat PFT protein also, the lectin domains seem to be involved in the recognition of the fungal pathogens. However, instead of kinase domains, here,

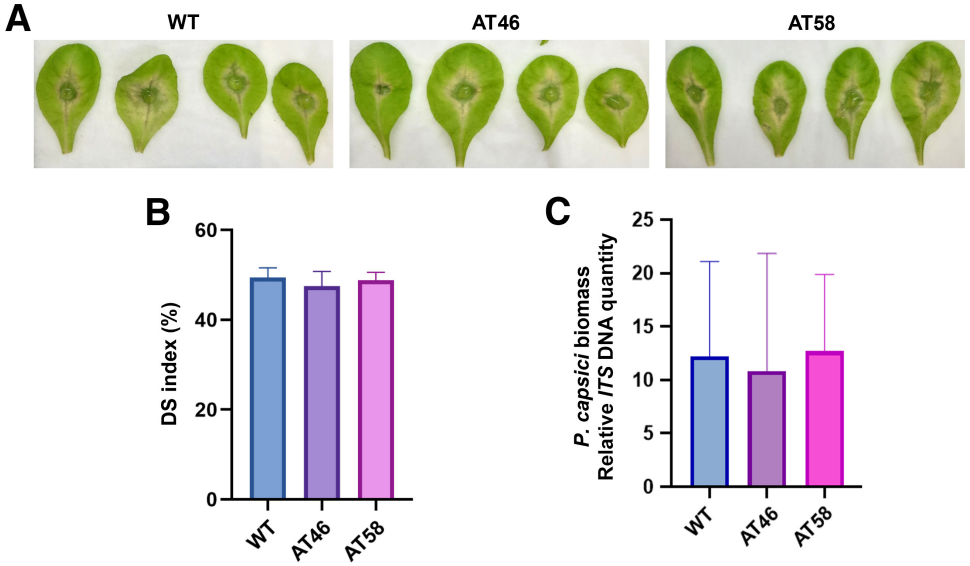

Fig. 6. Disease evaluation of wild type (WT) and transgenic T_2 *Arabidopsis* plants expressing GFP:PFT after oomycete (*Phytophthora capsici*) infection. **A,** Disease symptoms observed 3 days postinoculation (dpi) and **B,** disease severity (DS) index of WT and T_2 *Arabidopsis* leaves with *P. capsici*. **C,** Biomass of *P. capsici* detected by quantitative real-time PCR on inoculated leaves 3 dpi. Relative DNA quantity of the internal transcribed spacer region gene (*ITS*) was measured, using the by $2^{-\Delta CT}$ method, by normalizing data with the *Arabidopsis UBC* gene. WT is WT *Arabidopsis* Ler, and AT46 and AT58T_2 are *Arabidopsis* Ler families expressing GFP:PFT. Data represent means with standard error from four biological replicates. One or two asterisks (* or **) indicate that corresponding data is statistically different from WT at $P < 0.05$ or $P < 0.01$, respectively.

the lectin domains are fused to a bacterial toxin domain toward the 'C' terminus of the protein. How the toxin domain functions in the overall PFT protein activity is an important question that needs further exploration.

Previously characterized atypical BSR genes in wheat conferring resistance against multiple pathogens of different races or species belong to various classes, including membrane-associated pattern recognition receptors and transporters, NLR proteins with integrated domains, defense signaling proteins, sucrose transporters, and nonhost resistance proteins (Li et al. 2020; Sinha et al. 2022). The present work adds PFT to this list of atypical resistance proteins that can be transferred to a wide range of plant systems for effective resistance against a number of fungal pathogens. Further domain dissection and domain swapping studies could help in a better understanding of the mechanism of BSR conferred by PFT, further broadening its application.

Materials and Methods

Phylogenetic tree construction.

Protein sequences of different wheat PFT orthologs were retrieved from Phytozome-13 (https://phytozome-next.jgi.doe.gov/). Different monocots (*Triticum aestivum*, *Zea mays*, *Oryza sativa*, *Musa acuminate*, *Hordeum vulgare*, *Brachypodium distachyon*) and eudicots (*Arabidopsis thaliana*, *Vitis vinifera*, *Solanum lycopersicum*, *Solanum tuberosum*, *Ricinus communis*, *Populus deltoids*, *Phaseolus vulgaris*, *Medicago truncatula*, *Gossypium hirsutum*, *Glycine max*, and *Beta vulgaris*) were used as target species. Sequences were downloaded and aligned and alignments were analyzed by the neighbor-joining method in MEGA-X software version 11.0 (Tamura et al. 2021).

Protein cloning of PFT into a plant expression vector and plant transformation.

RNA was extracted from the wheat cultivar Sumai 3 and full-length PFT was amplified and cloned into entry vector pDONR221, using Gateway BP clonase reaction. PFT was fused with enhanced GFP at the N terminus and was cloned into plant expression destination vector pK7FWG2, using LR clonase reaction (Karimi et al. 2002). The expression of the GFP:PFT fusion construct was driven by the 35S CaMV promoter. After confirmation with Sanger sequencing, the GFP:PFT fusion construct was electroporated in *Agrobacterium tumefaciens* GV3101, which was used for transforming *Arabidopsis thaliana* ecotype Ler, using the floral dip method (Clough and Bent 1998). T_0 seeds were plated on Murashige-Skoog media with kanamycin (50 mg/liter), and the resistant T_1 plants were

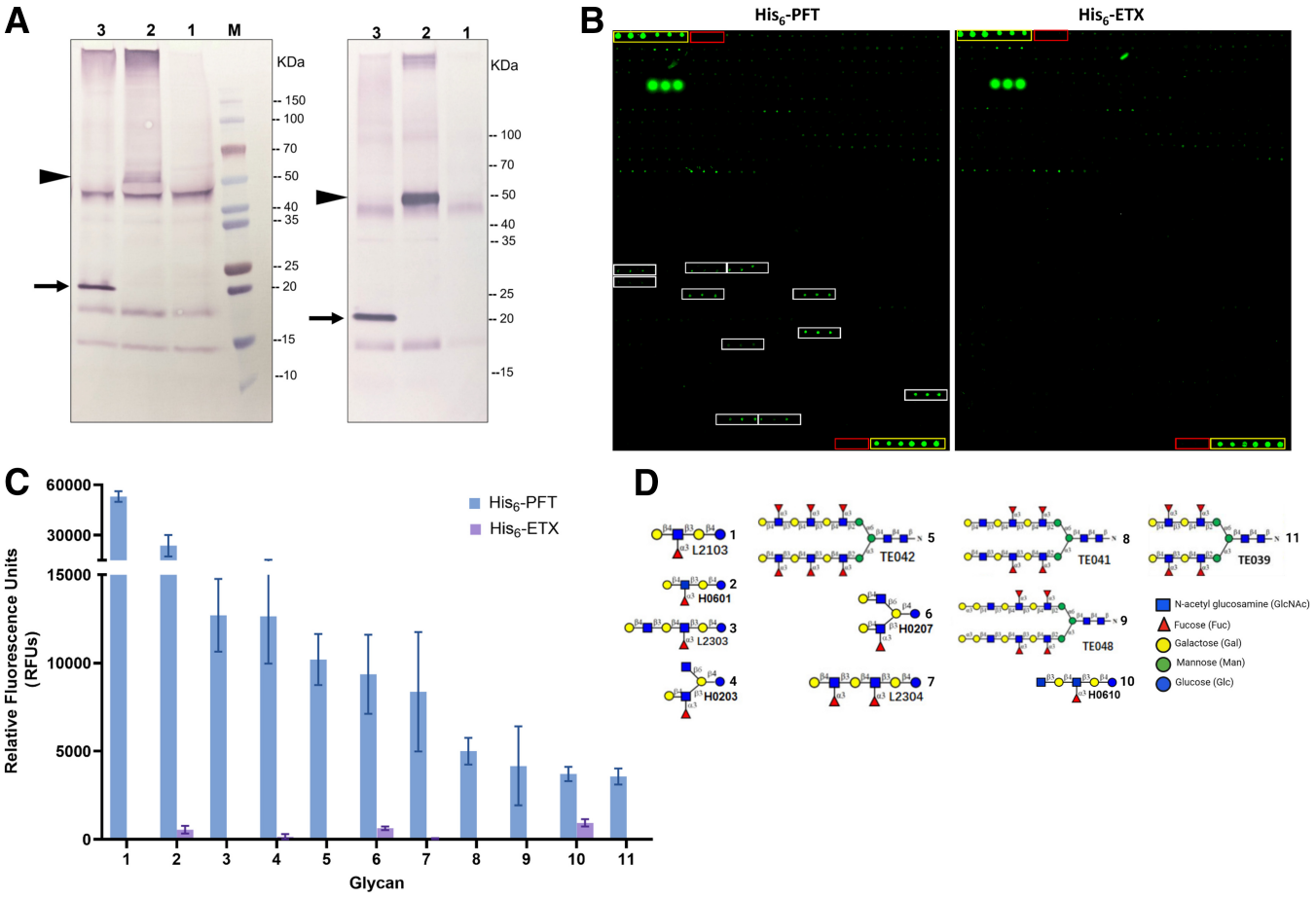

Fig. 7. Confirmation and binding of His6-PFT and His6-ETX to Glycan array 300. **A,** Western blot analysis of His6-PFT and His6-ETX expressed in *Nicotiana benthamiana*. On the left, immunoblots of soluble fractions of p19 (column 1), His6-PFT (column 2), and His6-ETX (column 3) after protein extraction. On the right, immunoblots of purified elution fractions of p19, His6-PFT, and His6-ETX (columns 1, 2, and 3, respectively) after affinity chromatography with Ni-NTA resins. Membranes were incubated with a monoclonal anti-His antibody followed by AP conjugated goat anti-mouse immunoglobulin G. M = ProSignal full-range prestained protein ladder. Arrowheads indicate the His6-PFT band and arrows indicate the His6-ETX band. **B,** Binding patterns of His6-PFT and His6-ETX on the Glycan array 300. Yellow box and red boxes highlight positive and negative controls, respectively. White boxes highlight specific binding of His6-PFT. **C,** Mean relative fluorescent units (± standard error of the mean) of 11 of the 300 glycans specifically binding to His6-PFT. **D,** Identities and structure of glycans specifically binding to His6-PFT with the highest affinity.

further screened for GFP signal, using a Nikon Eclipse epifluorescence microscope. T_1 plants were grown to produce T_2 seeds, which were further selected for homozygous individuals. Two independent homozygous T_2 families were used for disease assays. Further, four T_3 plant families were further selected on kanamycin-supplemented media and for GFP fluorescence and were subsequently used for disease assays.

Pathogen inocula preparation.

The fungi used for the study were *F. graminearum* GZ3639, *C. higginsianum*, *S. sclerotiorum*, and *B. cinerea* B05-10. Macroconidial inoculum of *F. graminearum* was prepared at a concentration of to 5×10^5 spores per milliliter, as described in Chhabra et al. (2021). Conidia production from *C. higginsianum* was induced on oatmeal agar and the spores were harvested after 7 days and were diluted, to a concentration of 5×10^5 spores per milliliter, using sterile water. For *S. sclerotiorum* inoculations, the fungal mycelia were grown on potato dextrose agar at room temperature, and mycelial plugs of 5 mm diameter taken from 7-day-old culture were used as inoculum. *B. cinerea* was grown on potato dextrose agar plates for 9 days, after which the spores were harvested and their concentration adjusted to 5×10^5 spores per milliliter in sterile water with 0.02% Tween-20.

Oomycete pathogen *Phytophthora capsici* was cultured in the dark at 25°C on 20% (vol/vol) V8 juice agar plates. Zoospores for plant inoculations were obtained by incubating mycelial plugs from the margin of a 4-day-old growing colony in 10% (vol/vol) cleared V8 broth in the dark at 25°C for 2 days. The V8 medium was then replaced with sterilized water and was incubated under continuous light 25°C for 2 days to get numerous sporangia. Zoospore release was induced with a cold shock by incubating at 4°C for 2 hr. Zoospores were filtered through a cheesecloth and were adjusted to 5×10^5 zoospores per milliliter.

Pseudomonas syringae pv. *tomato* DC3000 bacterial cells were grown at 28°C on Luria-Bertani (LB) medium supplemented with 100 μg of rifampicin per milliliter and 50 μg of kanamycin per milliliter. Bacterial suspensions of 1×10^8 CFU/ml were prepared in 10 mM $MgCl_2$, and 0.02% (vol/vol) Silwet L-77 for inoculations.

Disease assays on leaves.

Detached leaf assays for *F. graminearum*, *C. higginsianum*, *B. cinerea*, and an oomycete (*Phytophthora capsici*) were performed on leaves collected from rosettes of 4- to 5-week-old T_2 and T_3 generation transgenic and WT plants. Point injuries were made on the adaxial surface at the mid rib with a 10-μl pipette tip, and 5 μl of inoculum was deposited at the wounded site, after which the leaves were transferred to clear Petri plates with base lining of two to three layers of sterile wet Kimwipes. For *F. graminearum* inoculation, the inoculum was amended with 75 μM of deoxynivalenol (Sigma Aldrich). For the *S. sclerotiorum* assay, no mid-rib injury was made, and mycelial plugs of 5 mm diameter were directly placed with the fungal surface touching the adaxial surface of the detached *Arabidopsis* leaves on a Petri plate with base lining of two to three layers of sterile wet Kimwipes. The Petri plates were then sealed using parafilm and were placed in a dew chamber maintaining 100% relative humidity (RH) at 25°C and light intensity of 60 μmol m^{-2} s^{-1} with a 12-h light and 12-h dark cycle.

For bacterial assays, in planta infiltration inoculations as well as spray inoculations were conducted. The bacterial inoculum was infiltrated with a needle-less syringe into fully expanded leaves of 4-week-old *Arabidopsis* plants, after which the plants were kept in growth chambers under clear plastic domes for the first 24 h after treatment and were further incubated for 2 more days without plastic domes. For spray inoculations, whole rosettes of leaves of 4-week-old plants were sprayed with the bacterial inoculum, after which the leaves were detached and transferred to a Petri plate with a sterile lining of two to three layers of wet Kimwipes and were sealed with parafilm. In both assays, mock inoculations were done with 10 mM $MgCl_2$ and 0.02% Silwet L-77.

***F. graminearum* floral inoculations.**

Floral inoculations of the transgenic *Arabidopsis* plants were done following Urban et al. (2002), with a few modifications. Six-week-old plants with open flowers and developing siliques were spray inoculated with a macroconidial suspension with 1×10^5 spores per milliliter in sterile water with 0.001% Silwet L-77. Seven to ten puffs of fine spray were applied per inflorescence, while keeping the spray bottle at a 5-cm distance. The inoculated plants were kept in a large clear plastic box at 23°C for 7 to 8 days, with the base of the box filled with a 5-cm water depth to maintain 100% RH. For the first 2 days, plants were maintained in the dark by covering the box with black cover. On the fourth day, the lid was slightly opened to maintain approximately 80% RH.

Disease assessment.

Disease severity of detached leaf assays of all the fungal pathogens and oomycetes was assessed using two methods, the disease severity (DS) index and fungal or oomycete biomass. For the DS index measurement, images were collected at 5 dpi, for *F. graminearum*, *C. higginsianum*, *and B. cinerea*, 48 hpi for *S. sclerotiorum*, and 3 dpi for *Phytophthora capsici*. The disease was scored using a categorical rating system from 0 (resistant) to 5 (susceptible), as described by Chen et al. (2006). The disease scores were based on the symptom severity and scores were assigned as 0 = no symptoms, 1 = chlorosis/discoloration restricted to the site of inoculation, 2 = less than 25% area with chlorosis or discoloration, 3 = 25 to 50% area with chlorosis or discoloration, 4 = 50 to 75% area with chlorosis or discoloration, and 5 = 100% area with chlorosis or discoloration.

The DS index was calculated based on the following equation:

$$\left(\sum \mathrm{nSi}\right) / (\mathrm{NSm}) \times 100$$

where n is the number of leaves with each disease score (Si), N is the total number of leaves, and Sm is the maximum disease score possible (i.e., 5).

For PFT gene expression from transgenic lines and wild-type *Arabidopsis* plants, five plants of each type were used to collect leaf tissues (100 mg per plant), and RNA was extracted using the Trizol method. RNA quantity and purity were assessed by determining the A260/A280 ratio in a NanoDrop (Thermo Scientific). DNA contamination was removed from RNA samples, using TURBO DNase (Thermo Scientific) according to the manufacturer instructions. Complementary DNA (cDNA) was synthesized from 1 μg total RNA (DNase 1–treated), using the AzuraQuant cDNA synthesis kit (AzuraGenomics). The resulting cDNA was diluted five times and was used for qRT-PCR, using the AzuraView GreenFast qPCR blue mix LR (AzuraGenomics).

For fungal and oomycete biomass quantification, infected leaf samples from T_2, T_3 transgenic, and WT *Arabidopsis* plants were collected at 5 dpi for *F. graminearum*, *C. higginsianum*, and *B. cinerea*, 48 hpi for *S. sclerotiorum*, and 3 dpi for *Phytophthora capsici*. For the floral assays with *F. graminearum*, tissue was collected 8 dpi. DNA was extracted and normalized to 20 ng/μl and was used for qPCR with *Tri6*, *ITS2*, *Tubulin*, and *Cutinase A* as target genes for quantifying the DNA content of *F. graminearum* (Horevaj et al. 2011), *C. higginsianum* (Salvador-Guirao et al. 2018), *S. sclerotiorum* (Wei et al. 2022), and *B. cinerea* (Ono et al. 2020), respectively. Primer pair CAP-Fw/CAP-Rv

was used to target *Phytophthora capsici* ITS regions (Silvar et al. 2005; Wang et al. 2013). The *Arabidopsis* ubiquitin-conjugating enzyme (UBC) gene was used as a reference (Czechowski et al. 2005) (Supplementary Table S1). Primer efficiencies for the target and reference genes were in the range of 100 to 110%; therefore, DNA quantification data was analyzed using the $2^{-\Delta\Delta CT}$ method (Livak and Schmittgen 2001).

For bacterial biomass evaluation, the inoculated leaves were harvested 3 dpi, were ground to powder, followed by the addition of 500 µl of sterile 10 mM $MgCl_2$, and 20 µl of this suspension was transferred into the first row of a 96-well plate having 180 µl of 10 mM $MgCl_2$. A ten-fold serial dilution was prepared by transferring 20 µl of liquid into the next row and adding 180 µl of 10 mM $MgCl_2$, repeating this procedure until the sixth dilution. From each dilution, 10 µl of the suspension was transferred to an LB plate, which was then dried, inverted, and incubated at 28°C for 24 to 36 h, until the colonies were visible. Bacteria were counted under a stereozoom microscope before they overgrew and colonies fused. Number of CFU per square centimeter leaf) was determined using the formula

$$\text{CFU/cm}^2 \text{ leaf} = \left(\text{T} \times 10^{\text{R}}/20\right) \times 500/2$$

where T is the number of colonies and R is the dilution row in 96 well plate.

Trypan blue staining.

WT Ler and T_2 transgenic (AT46 and AT58) leaves inoculated with *F. graminearum* were collected 4 dpi for staining with trypan blue to reveal fungal growth and its effect in leaf tissue, as previously described (Lee et al. 2022). The leaves were cleared in acetic acid/ethanol (1:3, vol/vol) solution overnight, followed by clearing using acetic acid/ethanol/glycerol (1:5:1, vol/vol/vol) solution for 3 h. The tissue was then stained with trypan blue (0.01% trypan blue in lactophenol) overnight, was subsequently rinsed multiple times with distilled water, and was preserved in 60% glycerol, for microscopic observation using Nikon ECLIPSE.

PFT transient expression and protein extraction from *N. benthamiana* leaves.

For transient expression in *N. benthamiana*, full-length PFT cDNA and its agglutinin and ETX domains were amplified from the reverse-transcribed RNA of the wheat cultivar Sumai 3. His-tag (6x) was appended at the 5′ end of each of the amplicons, using primers listed in Supplementary Table S1, followed by directional TOPO cloning into the pENTR/D-TOPO vector (Invitrogen). The resulting His6-PFT, His6-Agg, and His6-ETX amplicons were cloned in a plant expression vector pGWB402 with a CaMV 35S promoter, using LR cloning reaction. pGWB402:His6-PFT, pGWB402:His6-Agg, and pGWB402:His6-ETX vectors were electroporated into *Agrobacterium tumefaciens* GV3101 cells, which were grown on LB agar containing rifampicin (25 µg/ml) and spectinomycin (50 µg/ml). The bacterial pellets were resuspended and gently shaken for 4 h at room temperature in an infiltration medium (10 mM $MgCl_2$, 10 mM MES, pH 5.7, 150 µM acetosyringone) at 0.7 optical density at 600 nm. Three to four fully expanded leaves of six-week-old *N. benthamiana* plants were infiltrated at the abaxial surface with a 1-ml needle-less syringe. The leaves were harvested, 4 days postinfiltration, by snap-freezing in liquid nitrogen. The leaf tissue was ground in liquid nitrogen and ice-cold protein extraction buffer (50 mM NaH_2PO4, pH 8.0, 300 mM NaCl, 10 mM imidazole, 10% glycerol) amended with 1 µM phenylmethylsulfonyl fluoride, and 0.5× Halt protease inhibitor cocktail was added to the ground leaf tissue at a 5:1 (buffer/tissue) ratio. The homogenate was centrifuged at 40,000 × *g* and 4°C for 30 min, and soluble protein fraction was collected as supernatant.

Protein purification using nickel resins (immobilized metal ion affinity chromatography) under native conditions and quantification.

To purify His6 tagged proteins, affinity purification was performed using Ni-NTA His-Bind resin and Ni-NTA buffer kit (Millipore Sigma). Fractions containing the proteins of interest were pooled and were concentrated using Amicon Ultra-4 centrifugal filters, with a 10-kDa cutoff (Millipore Sigma). The concentrated protein fraction was dialyzed against protein storage buffer (50 mM Tris-HCl, 1 mM $CaCl_2$, pH 8.0) overnight at 4°C, using a Slide-A-Lyzer mini dialysis device with a 10-kDa molecular-weight cutoff (ThermoFisher Scientific). Protein was quantified using a Pierce detergent-compatible Bradford assay kit, following the manufacturer protocol (ThermoFisher Scientific).

Protein gel electrophoresis and Western blot analysis.

Protein samples were mixed with Laemmli sample loading buffer and were heated at 95°C for 10 min, after which they were resolved on SDS-PAGE, using Novex Wedge Well 10% tris-glycine gels (Invitrogen), followed by Coomassie-based Simply Blue staining (Invitrogen). For immunodetection by Western blot, the proteins were blotted to a nitrocellulose membrane with a pore size of 45 µm (Invitrogen) using the XCell II blot module (Invitrogen). For blocking, the membrane was treated with 5% bovine serum albumin (BSA) in Tris-buffered saline (TBS; 20 mM Tris-HCl, 150 mM, pH 7.6) solution at room temperature for 2 h. The membrane was then probed with a 1:1,000 dilution of monoclonal anti-His antibody (Sigma Aldrich) in an antibody-diluting solution (TBS containing 0.1% Tween 20 and 2.5% BSA) overnight at 4°C. Subsequently, the membrane was washed three times with wash buffer (TBS containing 0.05% Tween 20), for 10 min each, and then, was treated with a 1:5,000 dilution of goat anti-mouse alkaline phosphatase-labeled immunoglobulin G in an antibody diluting solution for 2 h at room temperature (LGC SeraCare, Inc.). After three washes of 10 min each with wash buffer, the membrane was developed, using the BCIP/NBT alkaline phosphatase substrate system (LGC SeraCare, Inc.).

Glycan microarray analysis.

To determine the binding specificity of PFT, affinity-purified His6-PFT and His6-ETX fractions were screened against RayBio Glycan Array 300, which contains blocks of 300 synthetic glycan spots, in which each spot is replicated three times along with positive and negative control spots for normalization. Samples were biotinylated, and a label-based approach was used. Each sample was incubated with the array at a 2 µg/ml concentration. Data were normalized and analyzed using RayBio Analysis software. The glycan array screening and analysis was performed by RayBiotech.

Statistical analysis.

Data were analyzed using GraphPad Prism version 9.3.1 (GraphPad Software). Data sets were checked for the normality assumption, using Shapiro-Wilk test and Q-Q plots. One-way analysis of variance, followed by Dunnett's multi-comparisons test or Student's *t*-tests were performed for declaring statistical significance.

Acknowledgments

Authors are grateful to M. Bolton (United States Department of Agriculture-Agricultural Research Service, Fargo, North Dakota),

K. Everts (University of Maryland), T. Mengiste (Purdue University), and J. McDowell (Virginia Tech University) for kindly providing fungal and oomycete pathogens *Colletotrichum higginsianum*, *Sclerotinia sclerotiorum*, and *Botrytis cinerea* B05-10 and *Phytophthora capsici*, respectively, used for various inoculations. Authors are thankful for the excellent technical help provided by N. Kovalskaya for protein Western gels.

Literature Cited

Bartnicki-García, S. 1968. Cell wall chemistry, morphogenesis and taxonomy of fungi. Ann. Rev. Microbiol. 22:87-108.

Bentley, A. R., Donovan, J., Sonder, K., Baudron, F., Lewis, J. M., Voss, R., Rutsaert, P., Poole, N., Kamoun, S., Saunders, D. G. O. D. H., Hughes, D. P., Negra, C., Ibba, M. I., Snapp, S., Sida, T. S., Jaleta, M., Tesfaye, K., Becker-Reshef, I., and Govaerts, B. 2022. Near- to long-term measures to stabilize global wheat supplies and food security. Nat. Food 3:483-486.

Buerstmayr, M., Steiner, B., and Buerstmayr, H. 2020. Breeding for Fusarium head blight resistance in wheat—Progress and challenges. Plant Breed. 139:429-454.

Chen, X., Steed, A., Harden, C., and Nicholson, P. 2006. Characterization of *Arabidopsis thaliana-Fusarium graminearum* interactions and identification of variation in resistance among ecotypes. Mol. Plant Pathol. 7:391-403.

Chhabra, B., Tiwari, V., Gill, B. S., Dong, Y., and Rawat, N. 2021. Discovery of a susceptibility factor for Fusarium head blight on chromosome 7A of wheat. TheorAppl Genet. 134:2273-2289.

Chavonet, E., Gaucher, M., Warneys, R., Bodelot, A., Heintz, C., Juillard, A., Cournol, R., Widmalm, G., Bowen, J. K., Hamiaux, C., Brisset, M.-N., and Degrave, A. 2022. Search for host defense markers uncovers an apple agglutination factor corresponding with fire blight resistance. Plant Physiol. 188:1350-1368.

Clough, S., and Bent, A. 1998. Floral dip: A simplified method for *Agrobacterium*-mediated transformation of *Arabidopsis thaliana*. Plant J. 16:735-743.

Couto, D., and Zipfel, C. 2016. Regulation of pattern recognition receptor signalling in plants. Nat. Rev. Immunol. 16:537-552.

Czechowski, T., Stitt, M., Altmann, T., Udvardi, M., and Scheible, W. 2005. Genome-wide identification and testing of superior reference genes for transcript normalization in *Arabidopsis*. Plant Physiol. 139:5-17.

Dang, L., and Van Damme, E. J. M. 2016. Genome-wide identification and domain organization of lectin domains in cucumber. Plant Physiol. Biochem. 108:165-176.

Dangl, J. L., Horvath, D. M., and Staskawicz, B. J. 2013. Pivoting the plant immune system from dissection to deployment. Science 341: 746-751.

De Coninck, T., and Van Damme, E. 2021. Review: The multiple roles of plant lectins. Plant Sci. 313:111096.

Dodds, P. N., and Rathjen, J. P. 2010. Plant immunity: Towards an integrated view of plant-pathogen interactions. Nat. Rev. Genet. 11:539-548.

FAOSTAT 2020 Crop production summary. Food and Agriculture Organization of the United Nations, Rome. https://www.fao.org/faostat/en/#data/QCL (Accessed Oct 20, 2022).

Faruque, K., Begam, R., and Deyholos, M. K. 2015. The amaranthin-like lectin (LuALL) genes of flax: A unique gene family with members inducible by defense hormones. Plant MolBiol Rep. 33:731-741.

Franck, C. M., Westermann, J., and Boisson-Dernier, A. 2018. Plant Malectin-Like Receptor Kinases: From Cell Wall Integrity to Immunity and Beyond. Ann Rev Plant Biol. 69:301-328.

Goldman, R. C., and Branstrom, A. 1999. Targeting cell wall synthesis and assembly in microbes: Similarities and contrasts between bacteria and fungi. Curr. Pharm. Design 5:473-501.

Goswami, R. S., and Kistler, H. C. 2004. Heading for disaster: Fusarium graminearum on cereal crops. Mol. Plant Pathol. 5:515-525.

Hardham, A. R. 2007. Cell biology of plant-oomycete interactions. Cell. Microbiol. 9:31-39.

Horevaj, P., Milus, E., and Bluhm, B. 2011. A real-time qPCR assay to quantify *Fusarium graminearum* biomass in wheat kernels. J. Appl. Microbiol 111:396-406.

Jones, J. D. G., and Dangl, J. L. 2006. The plant immune system. Nature 444:323-329.

Karimi, M., Inzé, D., and Depicker, A. 2002. GATEWAY™ vectors for *Agrobacterium*-mediated plant transformation. Trends Plant Sci. 7: 193-195.

Kou, Y., and Wang, S. 2010. Broad-spectrum and durability: Understanding of quantitative disease resistance. Curr. Opin. Plant Biol. 13: 81-185.

Lee, S., Fu, F., Liao, C., Mewa, D., Adeyanju, A., Ejeta, G., Lisch, D., and Mengiste, T. 2022. Broad-spectrum fungal resistance in sorghum is conferred through the complex regulation of an immune receptor gene embedded in a natural antisense transcript. Plant Cell 34:1641-1665.

Li, W., Deng, Y., Ning, Y., He, Z., and Wang, G. L. 2020. Exploiting broad-spectrum disease resistance in crops: From molecular dissection to breeding. Ann. Rev. Plant Biol. 71:575-603.

Livak, K., and Schmittgen, T. 2001. Analysis of relative gene expression data using real-time quantitative PCR and the $2^{-\Delta\Delta CT}$ method. Methods 25:402-408.

Manzano, S., Megias, Z., Martinez, C., Garcia, A., Aguado, E., and Chileh, T. 2017. Overexpression of a flower-specific aerolysin-like protein from the dioecious plant *Rumex acetosa* alters flower development and induces male sterility in transgenic tobacco. Plant J. 89:58-72.

McMullen, M., Bergstrom, G., De Wolf, E., Dill-Macky, R., Hershman, D., Shaner, G., and VanSanford, D. 2012. A unified effort to fight an enemy of wheat and barley: Fusarium head blight. Plant Dis. 96:1712-1728.

Moran, Y., Fredman, D., Szczesny, P., Grynberg, M., and Technau, U. 2012. Recurrent horizontal transfer of bacterial toxin genes to eukaryotes. Mol. Biol.Evol. 29:2223-2230.

Ning, Y., and Wang, G. L. 2018. Breeding plant broad-spectrum resistance without yield penalties. Proc. Natl. Acad. Sci. U.S.A. 115:2859-2861.

Ono, E., Mise, K., and Takano, Y. 2020. RLP23 is required for *Arabidopsis* immunity against the grey mould pathogen *Botrytis cinerea*. Sci. Rep-U.K. 10:13798.

Peumans, W. J., and Van Damme, E. J. 1995. Lectins as plant defense proteins. Plant Physiol. 109:347-352.

Puthoff, D. P., Sardesai, N., Subramanyam, S., Nemacheck, J. A., and Williams, C. E. 2005 Hfr-2, a wheat cytolytic toxin-like gene, is upregulated by virulent Hessian fly larval feeding. Mol. Plant Pathol. 6: 411-423.

Rawat, N., Pumphrey, M. O., Liu, S., Zhang, X., Tiwari, V. K., Ando, K., Trick, H. N., Bockus, W. W., Akhunov, E., Anderson, J. A., and Gill, B. S. 2016. Wheat Fhb1 encodes a chimeric lectin with agglutinin domains and a pore-forming toxin-like domain conferring resistance to Fusarium head blight. Nature Genet. 48:1576-1580.

Salvador-Guirao, R., Baldrich, P., Weigel, D., Rubio-Somoza, I., and Segundo, S., B. 2018.The microRNA miR773 is involved in the *Arabidopsis* immune response to fungal pathogens. Mol. Plant-Microbe Interact. 31:249-259.

Silvar, C., Duncan, J., Cooke, D., Williams, N., Díaz, J., and Merino, F. 2005. Development of specific PCR primers for identification and detection of *Phytophthora capsici* Leon. Eur. J. Plant Pathol. 112:43-52.

Sinha, A., Singh, L., and Rawat, N. 2022. Current understanding of atypical resistance against fungal pathogens in wheat. Curr. Opin. Plant Biol. 68:102247.

Sun, Y., Qiao, Z., Muchero, W., and Chen, J. G. 2020 Lectin receptor-like kinases: The sensor and mediator at the plant cell surface. Front. Plant Sci. 11:596301.

Takemoto, D., Hardham, A., and Jones, D. 2005 Differences in cell death induction by Phytophthora elicitins are determined by signal components downstream of MAP kinase kinase in different species of Nicotiana and cultivars of *Brassica rapa* and *Raphanus sativus*. Plant Physiol. 138: 1491-1504.

Tamura, K., Stecher, G., and Kumar, S. 2021 MEGA11: Molecular evolutionary genetics analysis version 11. Mol Bio. Evol. 38:3022-3027.

Tian, J., Xu, G., and Yuan, M. 2020. Towards engineering broad-spectrum disease-resistant crops. Trends Plant Sci. 25:424-427.

Tsaneva, M., and Van Damme, E. J. M. 2020. 130 years of plant lectin research. Glycoconjugate J. 37:533-551.

Urban, M., Daniels, S., Mott, E., and Hammond-Kosack, K. 2002. *Arabidopsis* is susceptible to the cereal ear blight fungal pathogens *Fusarium graminearum* and*Fusarium culmorum*. Plant J. 32: 961-973.

Vaid, N., Macovei, A., and Tuteja, N. 2013. Knights in action: Lectin receptor-like kinases in plant development and stress responses. Mol. Plant 6:1405-1418.

Van Damme, E., Barre, A., Rougé, P., and Peumans, W. 2004. Cytoplasmic/nuclear plant lectins: A new story. Trends Plant Sci. 9:484-489.

Wang, Y., Bouwmeester, K., van de Mortel, J., Shan, W., and Govers, F. 2013. A novel *Arabidopsis*–oomycete pathosystem: Differential interactions with *Phytophthoracapsici* reveal a role for camalexin, indole glucosinolates and salicylic acid in defence. Plant Cell Environ 36: 1192-1203.

Wei, W., Xu, L., Peng, H., Zhu, W., Tanaka, K., Cheng, J., Sanguinet, K., Vandemark, G., and Chen, W. 2022. A fungal extracellular effector inactivates plant polygalacturonase-inhibiting protein. Nature Commun. 13:2213.

Wu, J., Luo, X., Guo, H., Xiao, J., and Tian, Y. 2006. Transgenic cotton, expressing *Amaranthus caudatus* agglutinin, confers enhanced resistance to aphids. Plant Breeding 125:390-394.

Xin, Y., Xiangrong, Z., Mingju, Z., Wenchao, G., Yingchuan, T., and Qizhong, X. 2011. Transgenic potato overexpressing the *Amaranthus caudatus* agglutinin gene to confer aphid resistance. Crop Sci. 51: 2119-2124.

Yan, T., Zhou, Z., Wang, R., Bao, D., Li, S., Li, A., Yu, R., and Wuriyanghan, H. 2022. A cluster of atypical resistance genes in soybean confers broad-spectrum antiviral activity. Plant Physiol. 188:1277-1293.

Zhao, H., Wang, X., Jia, Y., Minkenberg, B., Wheatley, M., Fan, J., and Jia, M. H. 2018. The rice blast resistance gene *Ptr* encodes an atypical protein required for broad-spectrum disease resistance. Nat.Commun. 9:2039.

Zhou, J. M., and Zhang, Y. 2020. Plant immunity: danger perception and signaling. Cell 181:978-989.

Zipfel, C. 2014. Plant pattern-recognition receptors. Trends Immunol. 35:345-351.